MULTI-ANTENNA NONCOHERENT ML SYNCHRONIZATION FOR UWB-IR OUTDOOR CHANNELS

Enzo Baccarelli, Mauro Biagi, Cristian Pelizzoni, Nicola Cordeschi, Fabio Garzia
{enzobac, biagi, pelcris, cordeschi }@infocom.uniroma1.it, fabio.garzia@uniroma1.it

INFO-COM Dept., University of Rome "La Sapienza",
via Eudossiana 18, 00184 Rome, Italy. Ph. no. +39 06 44585471 FAX no. +39 06 4873330

ABSTRACT

This contribution focuses on the (up to date unexplored) topic of the Maximum-Likelihood (ML) noncoherent synchronization of Multi-Antenna transceivers working in faded environments and employing Ultra Wide Band Impulse Radio (UWB-IR) transmit technology. The noncoherent ML synchronizer is developed for the most performing transmit scheme (e.g., the SIMO one) and its performance are evaluated under both signal-acquisition and tracking operating conditions. The performance gain in the synchronization of UWB-IR signals arising by the utilization of the Multi-Antenna technology is also evaluated.

1. SYSTEM MODEL

Let us consider a baseband point-to-point UWB-IR MIMO wireless system impaired by slow-variant flat-fading phenomena and equipped with $N_t \geqslant 1$ transmit and $N_r \geqslant 1$ receive antennas. By assuming Non Line Of Sight (NLOS) application scenarios, as in [2,4] the path gain h_{ji} from transmit antenna i to receive antenna j may be modelled as a zero-mean unit-variance real Gaussian random variable[1] (r.v.) and the $(N_t \times N_r)$ path gains $\{h_{ji} \in \mathbb{R}^1, 1 \leqslant j \leqslant N_r, 1 \leqslant i \leqslant N_t\}$ may be considered mutually independent[2]. After considering a packet-transmission system where each packet to be communicated is composed by a (known to the receiver) trailer field, followed by header and payload fields, as in [6,9] we assume that timing acquisition must be performed at the beginning of each transmitted packet by exploiting the trailer field and then time-tracking is carried out over the remaining parts (e.g., header plus payload) of the packet. Since high-throughput Multi-Antenna WLANs are typically planned for low-mobility applications involving nomadic user' terminals, the corresponding MIMO channel may be considered quasi static [2]. Thus, since the above mentioned path gains $\{h_{ji}\}$ may be considered constant during the transmission of the trailer field, the (base-band real) signal $r_j(t)$ measured at the output of the j-th receive antenna over the time window $[-T_0, T_0]$ corresponding to the transmission of the trailer field may be modelled as

$$r_j(t) = \sum_{i=1}^{N_t} h_{ji} x_i(t+\tau) + n_j(t),\ t \in [-T_0, T_0],\ j = 1...N_r, \tag{1}$$

where τ is the *unknown* delay to be estimated, while $\{n_j(t) \in \mathbb{R}^1\}, j = 1...N_r$ are mutually independent zero-mean Gaussian white noises with unit two-sided power density spectrum (*e.g.*, $\mathcal{N}_0/2 = 1$ (watt/Hz)). About (1), we assume that the delay τ falls into the interval $[-\bar{\tau}_{max}, \bar{\tau}_{max}]$, where $\bar{\tau}_{max}$ is the maximum expected delay that may be evaluated in advance as in $\bar{\tau}_{max}$=R/c, where R(mt) is the coverage range of the system and c=3 $\times$ 10^8mt/sec is the light speed. Furthermore, $x_i(t)$ in (1) is the (real-valued base-band) signal radiated by i-th transmit antenna during the trailer phase, and, according to the following relationship

$$x_i(t) = \sqrt{\frac{\mathcal{E}}{N_t}} \sum_{m=-N_s/2}^{N_s/2} s^{(i)}(t - 4m\bar{\tau}_{max}),\ t \in [-T_0, T_0],\ i = 1..N_t, \tag{2}$$

we assume that $x_i(t)$ is composed by the train of $(N_s + 1)$ non overlapped pulses $\{s^{(i)}(t-4m\bar{\tau}_{max}), m = 0, \pm 1, ..., \pm N_s/2\}$ time-shifted apart by multiple of $4\bar{\tau}_{max}$. In particular, we assume that the base-band pulse $s^{(i)}(t)$ employed by i-th transmit antenna exhibits *unit-energy* and spans the time-interval $t \in [-\bar{\tau}_{max}, \bar{\tau}_{max}]$. As a consequence, in order to capture at the receiver side the overall energy conveyed by

[1] As it is known, the flat-fading assumption requires that the (half-power) bandwidth of the transmitted UWB pulse is below the coherence bandwidth of the MIMO channel. Although the bandwidth of the UWB pulse may be over 1GHz, for outdoor microcellular applications the flat-faded assumption may be considered reasonably met [4,11,12]. Some results about the optimized design of multi-path impaired UWB systems have been recently reported in [11]. In addition this channel model is also considered in [12] and it may be considered reasonable for UWB-IR (this transmission technique has been chosen by the IEEE 802.15.3a working group) when NLOS outdoor propagation scenario is taken into account.

[2] As pointed out, for example in [13], to be this assumption met in WLAN applications, it suffices an antenna spacing of the order of $\lambda/2$, where λ is the wavelength of the radiated UWB pulse evaluated at the center frequency of the corresponding spectrum.

the observed signals in (1), the corresponding time-window T_0 of the system must (at least) equate

$$T_0 = 2(1 + N_s)\bar{\tau}_{max}. \quad (3)$$

Finally, being $\mathcal{E}$ (joule) in (2) the total energy radiated by all N_t transmit antennas over the duration $2\bar{\tau}_{max}$ of each pulse, thus the resulting SNR per pulse γ measured at the output of *each* receive antenna equates $\gamma = \mathcal{E}$, *regardless* to the number N_t of employed transmit antennas. Before proceeding, it is worthwhile to stress that, since the duration of $s^{(i)}(t), i = 1...N_t$, is limited up to $[-\bar{\tau}_{max}, +\bar{\tau}_{max}]$, thus we have the following orthogonality property:

$$\int_{T_0}^{T_0} s^{(i)}(t - 4m\bar{\tau}_{max})s^{(i)}(t - 4l\bar{\tau}_{max} + \Delta)dt =$$

$$= \begin{cases} 1, \text{for } l = m \text{ and } \Delta = 0, \\ 0, \text{for } l \neq m \text{ and } \mid \Delta \mid \leqslant 2\bar{\tau}_{max}, \end{cases} \quad (4)$$

so that the $(1 + N_s)$ components of the train in (2) and their Δ-shifted versions are orthogonal over the system time-window $[-T_0, T_0]$.

2. THE CRAMER-RAO BOUND (CRB) FOR MIMO SIGNALING AND NON COHERENT SYNCHRONIZATION

Our first task is to compute the CRB on the synchronization error of the considered MIMO UWB-IR system, so to gain insight about the ultimate achievable performance of the synchronizer we develop in the following Section. For this purpose, after indicating as $\dot{s}^{(i)}(t)$, $\ddot{s}^{(i)}(t)$ the first and second time-derivatives of the pulse $s^{(i)}(t)$ respectively, let us denote as

$$\varepsilon_{ss}(i,j) \triangleq \int_{-T_0}^{T_0} s^{(i)}(t)s^{(j)}(t)dt, \quad (5)$$

$$\varepsilon_{\dot{s}s}(i,j) \triangleq \int_{-T_0}^{T_0} \dot{s}^{(i)}(t)s^{(j)}(t)dt \quad (6)$$

and

$$\varepsilon_{\dot{s}\dot{s}}(i,j) \triangleq \int_{-T_0}^{T_0} \dot{s}^{(i)}(t)\dot{s}^{(j)}(t)dt, \leqslant i,j \leqslant N_t, \quad (7)$$

the resulting cross energies[3]. Afterwards, let us indicate as $\mathbf{Q}_0$ the symmetric semidefinite-positive $(N_t \times N_t)$ matrix whose (i,j)-th entry is $\varepsilon_{ss}(i,j)$, while $\mathbf{Q}_1$ denotes the corresponding $(N_t \times N_t)$ matrix with (i,j)-th entry equal to $\varepsilon_{\dot{s}s}(i,j)$. Finally, let be $\mathbf{Q}_2$ the $(N_t \times N_t)$ symmetric definite-positive matrix with the (i,j)-th given by $\varepsilon_{\dot{s}\dot{s}}(i,j)$.

[3]Obviously, $\varepsilon_{\dot{s}s}(i,i) = 0$ for any i, while $\varepsilon_{ss}(i,i) = 1$ for any i due to the above assumption of unit-energy pulses.

Thus, under the assumption that the receiver is fully unaware about actual values assumed by the MIMO channel coefficients $\{h_{ji}\}$, the CRB for the (unbiased) estimate of the delay parameter τ assumes the following form

$$\sigma_\epsilon^2(\tau) \triangleq \mathrm{E}\{(\tau - \hat{\tau})^2\} \geqslant \left\{ \left(\frac{\gamma(1 + N_S)}{N_t} \right)^2 N_r \cdot \right.$$

$$\left. \cdot \mathrm{Tra} \left\{ \left[\mathbf{Q}_2\mathbf{Q}_0^T - \mathbf{Q}_1\mathbf{Q}_1^T \right] \left[\mathbf{I}_{N_t} + \frac{\gamma(1 + N_S)}{N_t}\mathbf{Q}_0 \right]^{-1} \right\}^{-1} \right\} (\text{sec.}^2), \quad (8)$$

where the expectation in (8) is referred to to joint pdf of the received signals in (1) conditional on the actual value τ assumed by the delay parameter. Therefore, after accounting for the energy constraints $\varepsilon_{ss}(i,i) = 1$ and $\varepsilon_{\dot{s}s}(i,i) = 0$ (see Note 3), it can be viewed that the above bound depends on the

$$N_t(2N_t - 1) \quad (9)$$

values assumed by the cross-energies constituting the entries of the $\mathbf{Q}_0, \mathbf{Q}_1, \mathbf{Q}_2$ matrices. Hence, from a system design perspective, the key-problem is to set these cross-energies so to *minimize* the value assumed by the CRB in (8) that it is equivalent to design the optimized MIMO signaling format for the estimation of the delay parameter. Unfortunately, at the present this problem seems to resist closed-form analytical solution, even in the simpler case of $N_t = 2$ transmit antennas (additional details can be found in [10]).

3. ML DELAY ESTIMATION FOR SIMO SYSTEMS

The ML estimate $\hat{\tau}_{ML}$ of the delay parameter τ affecting the SIMO system is given by the following (definitory) relationship

$$\hat{\tau}_{ML} \triangleq \underset{\tau \epsilon [-\bar{\tau}_{\max}, \bar{\tau}_{\max}]}{\arg\max} \{\lg\ p(\underline{r}_1, .., \underline{r}_{N_t} \mid \tau)\}$$

$$\overset{(a)}{=} \underset{\tau \epsilon [-\bar{\tau}_{\max}, \bar{\tau}_{\max}]}{\arg\max} \left\{ \sum_{j=1}^{N_r} \left(\sum_{m=-N_s/2}^{N_s/2} \int_{-T_0}^{T_0} r_j(t)s(t - 4m\bar{\tau}_{max} + \tau)dt \right)^2 \right\}. \quad (10)$$

Since at medium-low SNR γ the pdf in (10) does no assume the exponential form reported by eq. (IV.C.32) on [5], we conclude that at medium-low SNRs the performance of the ML estimate in (10) does not achieve the Cramer Rao Bound (CRB) (see [10],[5,p.177] for more details on this general question).

3.1. The ML equation

By equating to zero the first derivative of pdf in (10) we obtain the so-called ML equation for the SIMO system in

(10) and it assumes the following form:

$$\sum_{j=1}^{N_r}\sum_{k=-N_s/2}^{N_s/2}\sum_{l=-N_s/2}^{N_s/2}\left(\int_{-T_0}^{T_0} r_j(t)s(t-4k\bar{\tau}_{max}+\tau)dt\right)\cdot$$

$$\cdot\left(\int_{-T_0}^{T_0} r_j(t)\dot{s}(t-4l\bar{\tau}_{max}+\tau)dt\right)=0. \qquad (11)$$

Before using (11) for computing the ML estimate $\hat{\tau}_{ML}$ defined in (10) we should ascertain that $\hat{\tau}_{ML}$ is the *unique* solution of (11). For sake of brevity this result is not reported here but it can be found in the Appendix III of [10].

Remark 1-On the shape of the employed pulse

The most adopted (unit-energy) pulse $s(t)$ in current UWB-IR data transmission systems is modelled as the second derivative of the Gaussian function and then it is formally defined as in [8]

$$s(t)\equiv\sqrt{\frac{8}{3T_s}}\left[1-4\pi\left(\frac{t}{T_s}\right)^2\right]\exp\left(-2\pi\left(\frac{t}{T_s}\right)^2\right), \qquad (12)$$

where T_s(sec) is the so-called "shaping factor" of the pulse. Now, for $\Delta\neq 0$ the autocorrelation and cross-correlation function of this pulse:

$$\rho_{ss}(\Delta) = \frac{1}{12}\exp\left(-\pi\left(\frac{\Delta}{T_s}\right)^2\right)H_4\left(\sqrt{\pi}\frac{|\Delta|}{T_s}\right),$$

$$\chi_{s\dot{s}}(\Delta) = \frac{1}{12\sqrt{2}}\exp\left(-\pi\left(\frac{\Delta}{T_s}\right)^2\right)H_5\left(\sqrt{\pi}\frac{\Delta}{T_s}\right),$$

vanish in the correspondence of the zeros of the 4-th and 5-th order Hermite polynomials $H_4(.)$ and $H_5(.)$. Thus it should be (carefully) checked that both no zero of $H_4(.)$ falls in the interval $[-2\bar{\tau}_{max}, 2\bar{\tau}_{max}]$ and only the zero at $\Delta=0$ of $H_5(.)$ falls in the interval. Otherwise, the above stated convergence property of the solution of the ML equation is no longer guaranteed.

4. THE NON COHERENT ML SYNCHRONIZER

An appealing feature of the ML equation (10) is that, in practice, it may be implemented via a suitable "Early-Late Gate" architecture. Specifically in the Appendix IV of [10] it is proved that the ML equation in (10) may be equivalently rewritten as

$$e(\hat{\tau})=0, \qquad (13)$$

where the error signal $e(\hat{\tau})$ depends on the current estimate output by the synchronizer and it is defined as

$$e(\hat{\tau})\triangleq-\sum_{j=1}^{N_r}\left[\left(\int_0^{2T_0} r_j(t+T_0)v(t+\hat{\tau})dt\right)+\right.$$

$$+\left(\int_0^{2T_0} r_j(t+T_0)v(t+\hat{\tau}-\mu)dt\right)+$$

$$+\sum_{j=1}^{N_r}\left(\int_0^{2T_0} r_j(t+T_0)v(t+\hat{\tau})dt\right)+$$

$$\left.+\left(\int_0^{2T_0} r_j(t+T_0)v(t+\hat{\tau}+\mu)dt\right)\right], \qquad (14)$$

where

$$v(t)\triangleq\sum_{k=1}^{1+N_s} s(t+4k\bar{\tau}_{max}-2\bar{\tau}_{max}), \qquad (15)$$

being the reference signal and μ (sec.) representing the early-late offset parameter. The first and second summations in (14) are the outputs of the "late" and "early" gates, respectively. A block diagram of the resulting synchronizer is reported Fig.1.

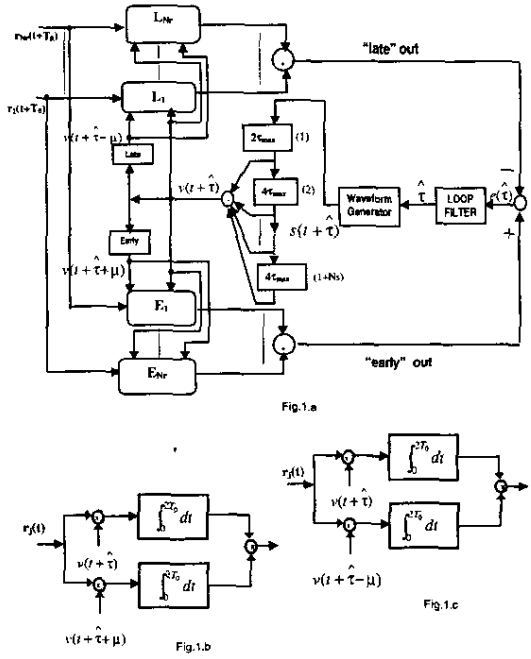

Fig. 1. (a) Block diagram of the overall noncoherent ML synchronizer. (b) Block diagram of j-th correlator of the Early Gate. (c) Block diagram of j-th correlator of the Late Gate.

4.1. The loop filter

From an implementation point of view, the proposed early-late gate synchronizer is composed by a tapped-delay-line

built up by $(1+N_S)$ elements whose outputs are combined to feed two banks of N_r correlating blocks. In turn, each correlating block is composed by two analog correlators (see Figs.1.b, 1.c), so that $4N_r$ analog correlators are required to implement the synchronizer. Although analog or digital Loop Filters (LFs) could be employed for updating the reference signal $v(t+\hat{\tau})$ of Fig.1.a, nevertheless, according to an ongoing technological trend, in the carried out numerical tests we have implemented first and second-order digital LFs to check the synchronizer performance.[4] Thus, after indicating as $e(m)$ and $\hat{\tau}(m)$ the input and output samples of the LF at the m-th iteration (e.g., at the instant $t = mD$), the input/output relationship for the 1-st order LF is [14]

$$\hat{\tau}(m) = \hat{\tau}(m-1) + G_0 e(m),$$

while for the 2-nd order LF we have [14]

$$\hat{\tau}(m) = 2\hat{\tau}(m-1) - \hat{\tau}(m-2) + (G_1+G_2)e(m) - G_1 e(m-1).$$

About the optimized setting of the filter coefficients G_0, G_1, G_2, we have tuned them according to the Jury's stability criterion [3], so to give arise to LFs with stable close-loop Transfer Functions.

5. SIMULATION SETUP AND NUMERICAL RESULTS

To test the performance of the proposed synchronizer we have adopted the (unit-energy) monocycle in (12) as transmitted pulse $s(t)$ with a shaping factor T_s of 2.99ns, so that the resulting frequency spectrum of the pulse spans about 1.43 GHz around the 1.1 GHz center frequency [1,8]. Values of $\bar{\tau}_{max}$ up to 50ns have been considered and the early-late offset μ has been set to 0.15ns. In addition, since the effect of the number $(1+N_S)$ of transmitted pulses in (7) is to amplify the SNR γ by the factor $(1+N_S)$ (see eq.(8)), thus, without loss of generality, $N_S = 2$ has been considered in the simulated setup. Finally, the (numerically evaluated) performance plots we report in the next sub-Sections have been averaged over 10^4 independent records of the fading coefficients $\{h_{j1},\ j=1,...,N_r\}$ of the SIMO channel. The performance of the proposed synchronizer has been checked under both signal-acquisition and tracking operating conditions.

5.1. Signal Acquisition

In this operating condition the actual value τ of the delay parameter has been randomly generated over the interval $[-\bar{\tau}_{max}, \bar{\tau}_{max}]$ and then held constant up to convergence of the synchronizer. The plots of Fig.2 allow the comparison of the (numerically) evaluated mean squared error performance of the synchronizer of Fig.1 against the corresponding CRB in (8) for increasing values of the number N_r of the receive antennas. These plots confirm that, even in the worst case of $N_r = 1$, SNRs γ of the order of 6.5dB suffice to achieve the CRB. Furthermore, for growing γ the convergence rate of the synchronizer performance toward the CRB increases by increasing the number N_r of the receive antennas, so that, for $N_r = 6$, SNRs less than 5dB suffice to achieve the CRB. Obviously, the steady-state performance reported in Fig.2 does not depend on the order of the employed LF. However, we expect that the time (e.g., the number of iterations) required by the 2-nd order LF for achieving the convergence is below than the corresponding one demanded by the 1-st order LF. By fact, the plots of Fig.3 confirm this conclusion and show that, at SNRs γ around 10dB, the convergence time of the 2-nd order LF is about one-half that of the 1-st order one.

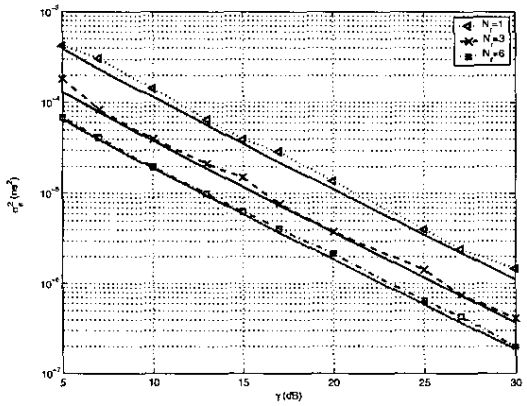

Fig. 2. Simulated mean squared errors of the synchronizer of Fig.1 (dashed lines) versus the corresponding CRBs (continuous lines):

5.2. Tracking

In order to test the tracking performance of the proposed synchronizer, as in [1] we have modelled the jitter-affected delay parameter as a (stationary) zero-mean Gaussian random sequence $\{\tau(i)\}$, whose samples are generated at the (multiple of the) frame-period T_0 in (3) according to the following relationship:

$$\tau(i) = c\tau(i-1) + (1-c^2)w(i). \qquad (16)$$

The sequence $\{w(i)\}$ in (16) is zero-mean, white and Gaussian, with standard deviation $\bar{\tau}_{max}$, while the parameter $c \in$

[4] In order to updating of the $(1+N_S)$ outputs of the tapped-delay-line present in Fig.1.a, the delay D introduced by the LFs should be of the order of $2(1+N_S)\bar{\tau}_{max}$.

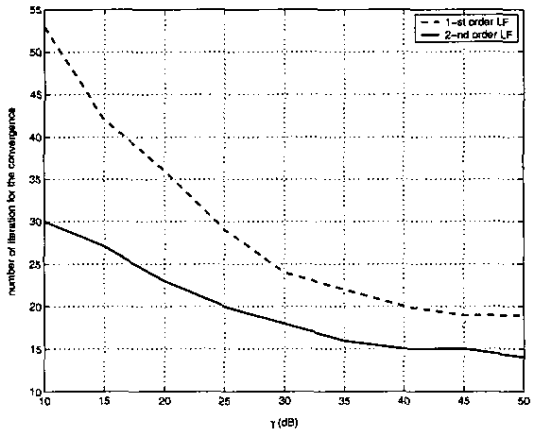

Fig. 3. Average number of iterations for the convergence of the 2-nd and 1-st order LFs systems with $N_r = 3$ receive antennas.

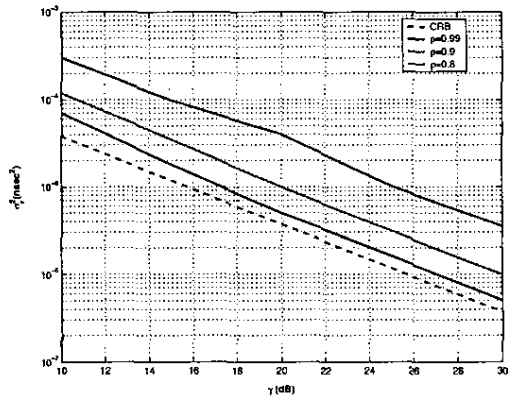

Fig. 4. Tracking performance of the proposed synchronizer equipped with the 1-st order LF. $I_{max} = 7$ and $N_r = 3$ have been considered .

$[-1, +1]$ is the correlation coefficient $\mathrm{E}\{\tau(i)\tau(i-1)\}/\mathrm{E}\{\tau^2(i)\}$ of the Markovian series $\{\tau(i)\}$. Therefore, c may be set according to the fluctuation rate desired for the jitter[5]. To evaluate the performance of the 1-st order LF, we have limited up to I_{max} the maximum number of iterations allowed the LF over each time-interval T_0, and the performance plots achieved for $I_{max} = 7$ have been drawn in Fig.4 for c = 0.99, 0.9 and 0.8 . As a benchmark, in Fig.4 we have also plotted the corresponding CRB in (8). In fact, since this last fixes the (ultimate) performance achievable by the synchronizer under signal-acquisition operating conditions, thus the gap between the simulated tracking performance and the CRB curves allows to evaluate both the performance loss induced by the jitter and the tracking capability of the proposed synchronizer.

6. REFERENCES

[1] W.M.Lovelace, J.K.Townsend, "The effects of Timing Jitter and Tracking on the Performance of Impulse Radio", IEEE JSAC, vol.20, no.9, pp.1646-1651, Dec.2002.

[2] E.Baccarelli, M.Biagi, C.Pelizzoni, P.F.Bellotti, "A Novel Multi-Antenna Impulse Radio UWB transceiver for Broadband High-Throughput 4G WLANs", IEEE Comm. Letters Vol.8, no.7, July 2004.

[3] E.I.Jury, "Theory and Application of the z-Transform Method", Wiley , N.Y., 1984.

[4] L.Yang, G.B.Giannakis, "Space-Time Coding for Impulse Radio", IEEE Conf. on Ultra Wideband Syst. and Techn., pp.235-239, May 2002.

[5] H.V.Poor, An Introduction to Signal Detection and Estimation, 2nd ed., Springer-Verlag, 1994.

[6] YYik-Chung Wu; E. Serpedin, "Data-aided maximum likelihood symbol timing estimation in MIMO correlated fading channels", ICASSP '04, 17-21 May 2004 pp.829-32 vol.4

[7] L.Yang, G.B.Giannakis, "Analog space-time coding for multiantenna ultra-wideband transmissions", IEEE Tr. on Comm., Vol.52, pp507-571, March2004.

[8] M.Win, R.A.Scholtz, "Ultra-wide bandwidth time-hopping spread-Spectrum impulse Radio for wireless multiple-access communications", IEEE Tr.On Comm., vol.48, pp.679-691, Apr.2000.

[9] R.A.Scholtz, "UWB radio deployment challenges" Proc. of IEEE PIMRC,pp.620-625, Sept.2000.

[10] E.Baccarelli, M.Biagi, C.Pelizzoni, P.Capogrosso "Noncoherent ML Synchronization of Multi-Antenna UWB-IR faded Systems", INFO-COM Tec. report, available at website *http : //infocom.uniroma1.it/~biagi/mimouwbsinc.pdf*

[11] M.Weisenhorn, W.Hirt, "Performance of binary antipodal signaling over indor UWB MIMO channel", IEEE International Conference on Communication (ICC) 2003, vol.4, pp.2872-2878, 11-15 May 2003.

[12] www.ieee802.org/15/pub/TG3a.html

[13] J.Salz, J.H.Winters, "Effects of fading correlation on adaptive arrays in digital Mobile Radio", IEEE Tr.on Vehic. Tech., pp.1049-1057, Nov. 1994.

[14] W.C.Lindsey, "A Survey of Digital Phase-Locked Loops", Proc.of IEEE, Vol.69, no.4, pp.410-431, Apr. 1981.

[5]Specifically, $c = 1$ gives arise to a maximally correlated time-invariant (e.g., jitter free) sequence, while for $c = 0$ the sequence $\{\tau(i)\}$ reduces to the white series $\{w(i)\}$. So, the fluctuation rate of the generated jitter increases by passing from $c = 1$ to $c = 0$.